The unique procoagulant adaptations of pseudonaja textilis venom factor V and factor X

Schreuder, M.

Chapter 4

Pseudonaja textilis Venom Factor Va Circumvents Natural Regulatory Mechanisms via a Unique A2 domain Region

Mark Schreuder, Ka Lei Cheung, Lynn Kruijsdijk, Pieter H. Reitsma, Mettine H.A. Bos

Manuscript in Preparation

Abstract

The coagulation factor V (FV) variant derived from the venom of the Australian snake Pseudonaja textilis (ptFV) has several unique procoagulant adaptations that circumvent the normal regulatory mechanisms in order to initiate coagulation in an uncontrolled manner. Interestingly, ptFV comprises a significantly extended A2 domain C-terminus (A2T), a region of which the role in human FV biology is poorly understood. In this study, we generated several chimeric FV variants to explore the functional relevance of this extended structural region. Surprisingly, our findings demonstrate that ptFV's enhanced procoagulant function is mediated by the A2T. Using this structural element, ptFV bypasses the need for membrane binding by facilitating productive interactions with P. textilis venom FXa and prothrombin in solution. Moreover, via a peptide-based approach we have established that the N-terminal region in the ptFV A2T plays a key role in the lipid-independent activity. Remarkably, substitution of the human A2T for the corresponding region in ptFV enabled human FVa to function in the absence of membranes, in a similar fashion to ptFVa. In addition, the ptFV A2T region was found to be of paramount importance for the functional activated protein C-resistance. Unlike in mammalian FVa, a ptFVa variant comprising the human FV A2T retained structural integrity despite loss of cofactor function. Taken together, the ptFV A2T represents an exceptional structural element responsible for the enhanced procoagulant functions that are at the basis of the snake venom's extreme toxicity.

Introduction

The coagulation cascade is composed of serine proteases and cofactors that act in a concerted manner to minimize blood loss following vascular injury. The regulatory mechanisms that strictly confine the activity of these coagulation proteins are of critical importance to maintain hemostasis. Intriguingly, the venom of various snake species comprises uniquely modified proteins that specifically act on coagulation pathways, aiming to disrupt the host's hemostatic system and incapacitate prey animals[1-4]. In humans, snake envenoming can lead to venom-induced consumptive coagulopathy (VICC), the most commonly observed clinical phenotype following envenomation in Australia[5]. VICC is characterized by uncontrolled activation of the coagulation system resulting in the consumption of fibrinogen, factors V and VIII, elevated D-dimer levels, and an international normalized ratio >3[6-8]. As a consequence, patients are at significantly increased risk for spontaneous and life-threatening hemorrhages[9].

Previously we, amongst others, reported that the FV(a)- and FX(a)-like proteins found in the venom of the Australian snake *Pseudonaja textilis* (ptFV[10,11] and ptFX[12,13], respectively) comprise several remarkable procoagulant adaptations that could be at the basis of the venom's potent toxicity[10,14,15]. ptFXa exhibits a reduced sensitivity towards antithrombin[16], in part due to extension of the 99-loop located directly adjacent to the active site[16,17]. Recently, we showed that the shortened ptFX activation peptide allows the zymogen form of ptFX to interact with the cofactor FVa and proteolytically convert prothrombin[18]. With respect to ptFV, it lacks the basic and acidic B-domain regions that keep FV in a procofactor state[19,20], thereby generating a constitutively active cofactor[14]. Moreover, ptFV has circumvented several negative regulatory pathways by bypassing the need for membrane binding and maintaining cofactor activity following activated protein C (APC)-dependent proteolysis[10,14]. For the latter we recently demonstrated that the ptFVa A2 domain loop2 facilitates stable A1-A2 domain interactions which likely prevent A2 domain dissociation following APC-proteolysis[21]. Despite this, the full molecular mechanism underpinning the procoagulant gain-of-functions of ptFV remains largely unexplained, suggesting that ptFV has developed other unique structural features to escape normal hemostatic regulation.

The characteristic acidic region hallmarking the A2 domain C-terminus (A2T) is significantly extended in ptFV relative to other FV species[10,11]. Although the functional role of the human FV A2T is poorly understood, previous reports have implicated the A2T in the formation of the prothrombinase complex and engagement of prothrombin[22-27]. In line with this, Shim *et al.* reported a complete 3D-model for the human prothrombinase–prothrombin complex, which revealed an extensive interaction

between the FVa A2T, the protease FXa, and substrate prothrombin[28]. Here we show that the ptFV A2T is responsible for the remarkable procoagulant enhancements of ptFV by facilitating productive interactions with ptFXa and prothrombin in the absence of membranes and following APC-proteolysis of the cofactor. As such, we have identified a unique structural element that gives ptFV the ability to promote uncontrolled blood clotting. These findings highlight the exceptional mechanism by which ptFV has been converted into a potent procoagulant weapon.

Materials and Methods

Construction and purification of FV variants: The construction, expression, and purification of FV variants are described in the Supplementary Information.

Macromolecular substrate activation: Steady-state initial velocities of macromolecular substrate cleavage were determined discontinuously at 25°C in assay buffer as described[17,29]. Briefly, progress curves of prothrombin were obtained by incubating PCPS (50 μM), DAPA (10 μM), and prothrombin (1.4 μM) with the recombinant FVa species (20 nM), and the reaction was initiated with 0.1–1 nM of hFXa or ptFXa upon which the rate of prothrombin conversion was measured[29].

APC-induced inactivation of FVa variants: FVa variants (500 nM) were incubated at 37°C with APC (10 nM for human FVa (hFVa); 750 nM for ptFVa) in the presence of PCPS (50 μM). Aliquots of the reaction mixtures were withdrawn at the indicated time intervals and analyzed by SDS-PAGE and via residual FVa cofactor activity assessment. FVa cofactor activity assay mixtures contained prothrombin (1.4 μM), PCPS (50 μM), DAPA (10 μM), hFVa (0.2 nM) or ptFVa (0.1 nM) variants and hFXa (2 nM) or ptFXa (1 nM), respectively. Prothrombin activation was determined as described under "Macromolecular substrate activation".

Peptide inhibition of prothrombinase-mediated prothrombin conversion: The inhibition of prothrombinase activity was measured continuously at 25°C in assay buffer. Assay mixtures containing prothrombin (1.4 μM), DAPA (10 μM), S2238 (100 μM), hFVa-ptA2T or ptFVa (5 pM), and peptides at indicated concentrations were incubated for 5 min at 25°C, and reactions were initiated with 1 nM ptFXa. The conversion of S2238 (100 μM) was followed for 60 min upon which the prothrombin conversion rate was measured[29].

Size-exclusion chromatography of APC-treated FVa variants: ptFVa-hA2T (500 μg) was subjected to APC (1 mM) treatment for 180 min at 37°C in the presence of

50 μM PCPS. Reactions were quenched by the addition of 50 μM PPACK and 1 mM benzamidine (BZA). A 10 mm × 300 mm column containing Superdex 200 Increase (Cytiva, Marlborough MA, USA) was equilibrated in assay buffer supplemented with 50 μM PPACK and 1 mM BZA. The 400 μL reaction mixture was applied to the column and eluted with equilibration buffer at a flow rate of 0.25 mL/min at room temperature. Fractions (0.25 mL) were collected and analyzed by SDS-PAGE.

Statistical analysis: All in vitro data are presented as mean ± 1 standard deviation and are the result of at least two to three independent experiments, unless otherwise stated.

Results

Generation of FV variants. The FVa A2T consists of an extended series of negatively charged amino acids with a currently unknown tertiary structure and poorly understood function. Sequence analysis revealed that ptFV comprises a significantly extended A2T (extended by 31 residues) compared to human FV (hFV) or other FV species, including that of several reptiles **(Fig. S1A)**. To examine the functional relevance of this extended region we created chimeric FV variants by exchanging the A2T between hFV and ptFV, resulting in hFV-ptA2T and ptFV-hA2T, respectively (**Figs. 1A**, **S1B**). The FV variants were stably expressed in BHK cells and purified to homogeneity by ion-exchange chromatography. Thrombin-activated FVa variants were subjected to SDS-PAGE under reducing **(Fig. 1B)** and non-reducing **(Fig. S2)** conditions. Each variant migrated on SDS-PAGE with the expected mobility; ptFV migrates as a single molecule under non-reducing conditions due to disulfide linkage of the A2-A3 domains[14,16].

Contribution of the ptFV A2T to prothrombinase assembly and prothrombin conversion. Previous studies have implicated the A2T as a FXa and/or prothrombin binding region[22-27], yet contradictory findings have been reported[30,31]. To assess the function of the extended ptFV A2T, we determined the kinetics for prothrombinase assembly by titration of the cofactor in the presence of hFXa/ptFXa and saturating amounts of anionic phospholipids. Similar to previously reported values[17,19,32,33], the apparent binding affinity of hFVa for hFXa was ~1.6 nM, **(Figure 2A; Table 1)**. hFVa-ptA2T displayed a near identical affinity for hFXa (~1.7 nM), indicating that the ptFV A2T does not significantly contribute to assembly of the human prothrombinase complex. Although the apparent affinity of the ptFVa variants for ptFXa was lower relative to those of the human system and to previously reported values[14,34], no differences were observed between ptFVa and ptFVa-hA2T **(Figure 2A; Table 1)**. Steady-state kinetic constants for prothrombin conversion revealed that in the presence of FXa the chimeric

FVa variants engaged prothrombin in a manner similar to the respective wild-type FVa species **(Figure 2B; Table 1)**. Conversely, the catalytic rates of prothrombin activation appeared modestly affected following exchange of the A2T between hFVa and ptFVa **(Figure 2B; Table 1)**. Nevertheless, the kinetic parameters were comparable to those earlier reported[14,17,31,34,35]. These findings may indicate that the ptFV A2T interacts with prothrombin in a different manner which could affect the orientation of the prothrombin activation sites towards FXa and as such the rate of catalysis.

The ptFV A2T facilitates macromolecular substrate conversion in the absence of anionic phospholipids. One of the procoagulant characteristics of ptFV is its unique ability to function in the absence of anionic membranes[14]. We next aimed to assess whether A2T plays a role in this gain-of-function feature. While the initial velocity of prothrombin activation was comparable between ptFVa and ptFVa-hA2T in the presence of anionic membranes, the velocity of prothrombin conversion by the ptFVa/ptFXa complex was 3.5-fold reduced in reaction mixtures lacking phospholipids **(Figure 3A)**. In contrast, the activity of the human FVa/FXa complex was virtually abolished in the absence of anionic membranes **(Figure 3B)**, consistent with previous findings[14]. Strikingly, upon exchange of the A2T, ptFVa-hA2T completely lost its ability to function in solution **(Figure 3A)**, indicating that the A2T is at the basis of ptFV's lipid-independent cofactor function. Following functional assessment of hFVa-ptA2T prothrombin conversion rates similar to hFVa were obtained in the presence or absence of anionic membranes when assayed with hFXa **(Figure 3B)**. However, as ptFX(a) comprises unique modifications that could contribute to the lipid-independent prothrombin conversion as well, the cofactor function of the human FVa variants was also assessed using ptFXa as protease. In the presence of ptFXa and phospholipids, hFVa-ptA2T exhibited a similar initial velocity of prothrombin conversion compared to hFVa **(Figure 3B)**. Remarkably, when anionic membranes were absent, the hFVa-ptA2T/ptFXa complex displayed a 24-fold increased rate of prothrombin conversion relative to hFVa/ptFXa **(Figure 3B)**, which was similar to that observed for the ptFVa/ptFXa complex **(Figure 3A)**. Comparable results were obtained using the chimeric variant hFVa-ptA2T-Y656C **(Figure S3A)** that comprises the complete ptFV A2T in which the highly conserved human Cys575-Cys656 disulfide bond is reintroduced **(Figs. 1A, S1B)**.

Importantly, these results could be explained by the contamination of phospholipids during purification, as described previously[36]. To remove putative lipid contaminants, FVa variants were treated with phospholipase C in the presence of phospholipids. Incubation with phospholipase C nearly abolished cofactor activity of hFVa and ptFVa-hA2T likely due phospholipid cleavage **(Figure S3B).** In contrast, the rate of prothrombin activation was markedly higher for the cofactors hFVa-ptA2T and ptFVa,

suggesting that the ptFV A2T is responsible for this unique lipid-independent activity. Further assessment of the lipid-independent prothrombin conversion as a function of the phospholipid concentration (0.05-100 μM) in the presence of ptFXa revealed similar initial rates of prothrombin conversion for hFVa and hFVa-ptA2T **(Figure 3C)**. However, phospholipid concentrations <0.05 μM had no appreciable effect on the rate of prothrombin activation with hFVa-ptA2T as cofactor, whereas the generation of thrombin was virtually undetected using hFVa **(Figure 3C)**. These results show that the lipid-independent effects exerted by the A2T become apparent in conditions with low phospholipid concentrations (<0.05 μM).

The ability of prothrombin to bind anionic membranes and thereby promote assembly of the prothrombinase-prothrombin complex might interfere with the interpretation of our results. To overcome this we determined the kinetics of prethrombin-1 conversion, which is a prothrombin derivative that lacks the kringle-1 and membrane binding Gla domains and does not interact with a lipid surface. Strikingly, using ptFXa as protease hFVa-ptA2T was able to activate prethrombin-1 both in the presence of anionic membranes and in solution phase with equivalent kinetic parameters, similar to ptFV **(Figure 3D, Table 1)**[14]. Conversely, prethrombin-1 conversion was absent in reaction mixtures with hFVa or ptFVa-hA2T as cofactor for ptFXa on membranes. Analysis of cleavage products of prothrombin and prethrombin-1 conversion by ptFV-ptFXa demonstrated that, similar to human prothrombinase, prothrombin conversion on anionic membranes proceeds through initial cleavage at Arg320, thereby forming the intermediate meizothrombin, and subsequent proteolysis at Arg271 resulting in the formation of thrombin and fragment 1.2 typical to the meizothrombin pathway **(Figure S4A)**[37]. Interestingly, we and others observed that in the absence of phospholipids ptFV-ptFXa proteolysis of prothrombin follows the opposite order of cleavage, generating the intermediates prethrombin-2 and fragment 1.2 via the prethrombin-2 pathway **(Figure S4B)**[16], similar to membrane-bound hFXa in the absence of cofactor[37]. In sharp contrast, prethrombin-1 proteolysis by ptFV-ptFXa proceeded via the prethrombin-2 pathway in the presence and absence of membranes **(Figure S4C,D)**. These observations indicate an important role for the substrate-membrane interaction in directing the order of substrate cleavage, consistent with findings by others[38]. Control experiments in the absence of $CaCl_2$ and with EDTA added to abolish any potential lipid binding as a consequence of residual lipid present in the protein preparations revealed significant prethrombin-1 conversion (**Table S1**).

Inhibition of the lipid-independent cofactor activity of ptFV-hA2T by peptide A2T fragments. To gain more insight into the mechanistic principles by which the ptFV A2T bypasses the need for membrane binding, we assessed the ability of three peptides

representing segments of the ptFV A2T (**Figure 4A**) to inhibit the lipid-independent activity of the hFVa-ptA2T/ptFXa complex in a continuous assay. Interestingly, in the absence of membranes addition of increasing concentrations of peptide 1 markedly reduced prothrombin activation **(Figure 4B)**. Conversely, peptide 2 exhibited a modest inhibitory effect **(Figure 4C),** whereas addition of up to 350 μM of peptide 3 had practically no impact on the lipid-independent prothrombin conversion **(Figure 4D)**. Comparable results were obtained using the ptFVa/ptFXa enzyme complex **(Figure S5)**. These data suggest that the Asp653-Ser681 sequence covered by peptide 1 and part of the Glu682-Leu709 sequence in peptide 2 could play a crucial role in the lipid-independent cofactor activity of ptFV.

The ptFV A2T plays a major role in the functional resistance to APC. In a recent study, we demonstrated that APC-mediated proteolysis of ptFVa at the essential cleavage sites equivalent to Arg306 and Arg506 had no appreciable effect on the cofactor activity[21], indicating that ptFV comprises unique structural elements that prevent inactivation. To further identify these, we assessed the functional consequences of APC-catalyzed proteolysis following A2T exchange between hFVa and ptFVa. SDS-PAGE analysis of APC-treated FVa variants revealed that ptFVa-hA2T was cleaved at the introduced human Arg679 cleavage site, whereas this cleavage was absent in ptFVa and hFVa-ptA2T **(Figure S6A-D)**. Evaluating the cofactor activity in a purified component assay showed that APC-proteolyzed ptFVa retained full cofactor activity upon a two hour incubation with APC **(Figure 4A)**, despite being fully proteolyzed **(Figure 5A)**. Intriguingly, a significant loss of cofactor activity was observed using APC-treated ptFVa-hA2T as cofactor **(Figure 4A)**. In case of the latter, the newly introduced human Arg679 cleavage site may be responsible for the loss of cofactor ptFVa-hA2T activity. To assess this, a chimeric ptFV variant comprising the Arg679Glu substitution was generated and analyzed (ptFVa-hA2T-R679Q, **Figure S1B**). Whereas ptFVa-hA2T displayed a ~75% loss of cofactor activity following APC-proteolysis, only a ~35% loss of activity was observed for APC-catalyzed ptFVa-hA2T-R679Q **(Figure 4A,S6E)**. Collectively, these findings suggest that the C-terminal region of ptFV A2T (Pro680-Arg740) plays an important role in the functional APC resistance.

Functional analysis of human FVa variants using hFXa revealed that hFVa-ptA2T was inactivated upon APC-mediated proteolysis in identical fashion to hFVa **(Figure 4B)**. We hypothesized that despite comprising the ptFV A2T, the APC-mediated inactivation resulted from proteolysis at the two major human APC cleavage sites in FVa, Arg306 and Arg506, whereas ptFVa is only targeted at the homologous Arg506 site[14]. To test this, the human Arg306 region in hFV-ptA2T was substituted for the corresponding ptFV region[21], generating hFV-ptA2T-pt306. Functional assessment revealed that hFVa-

ptA2T-pt306 retained ~50% cofactor activity following cleavage by APC **(Figure 4B)**, similar to previously reported FVa variants comprising an Arg306 mutation[39]. When APC-proteolyzed human FVa variants were assayed with ptFXa, the inactivation of hFVa-ptA2T was found to be slower relative to assessments in the presence of hFXa, indicating that ptFXa is able to support the cofactor function of APC-cleaved cofactor **(Figure 4B)**. Remarkably, APC-proteolyzed hFVa-ptA2T-pt306 maintained full cofactor activity in the presence of ptFXa **(Figure 4B,S6F)**. Furthermore, we generated a ptFVa molecule in which the human Arg306 region was introduced and ptFVa's unique disulfide bond connecting the A2-A3 domains was eliminated[21] (ptFVa-hA2T-h306-SS). Following a two hour incubation with APC, ptFVa-hA2T-h306-SS retained a similar activity (~15%) relative to ptFVa-hA2T **(Figure 4A,S6G)**, highlighting the extraordinary stability of ptFVa. As such, our findings demonstrate that the ptFV A2T and absence of the Arg306 cleavage site are of substantial importance for the functional APC-resistance of ptFV.

ptFVa-hA2T maintains structural integrity despite loss of cofactor function. Recently we demonstrated that ptFVa comprises stable non-covalent A2-A1 interactions that prevent A2 domain dissociation following APC-mediated proteolysis[21]. We next examined whether the loss of ptFVa-hA2T activity correlates with A2 domain dissociation. Following size-exclusion chromatography of APC-treated ptFVa-hA2T, elution fractions were analyzed by SDS-PAGE. In contrast to hFVa, APC-proteolyzed ptFVa-hA2T displayed a similar elution profile **(Figure 5A)** as proteolyzed ptFVa[21]. Furthermore, SDS-PAGE analysis revealed that ptFVa-hA2T eluted as a single complex, demonstrating that ptFVa-hA2T maintained structural integrity **(Figure 5B)**. These data therefore indicate that the loss of ptFVa-hA2T activity following APC-proteolysis is the result of a reduced affinity for ptFXa and/or prothrombin rather than A2 domain dissociation, corroborating our previous findings that non-covalent A2-A1 domain interactions in ptFVa are responsible for its unique structural integrity[21].

Discussion

The requirement for a negatively-charged phospholipid layer in support of enzymatic reactions is one of the hallmarks of coagulation and confines the procoagulant response to the site of injury while dramatically enhancing the enzyme assembly process[40,41]. Remarkably, ptFV has bypassed the need for membrane binding by forming a high affinity complex with ptFXa in solution[14]. This unique feature could potentially allow the systemic disruption of hemostasis upon envenomation. Our findings show that the ptFV A2T is responsible for this exceptional characteristic. This study thereby provides novel insights in the mechanistic role of the FVa A2T in the binding and conversion of prothrombin.

Previous studies into the functional role of the human FV A2T have reported contradictory results[22-26,31,33]. Here, we made use of a uniquely modified natural FV variant comprising an extended A2T. Functional characterization of chimeric FVa variants following A2T exchange between human and *P. textilis* FV revealed modest differences in the maximal prothrombin conversion rates at saturating conditions of membranes. The slightly reduced prothrombin activation rate in FVa variants comprising the ptFV A2T might reflect the use of human prothrombin and could indicate that the ptFV A2T interacts with prothrombin in a somewhat different and less efficient manner relative to the hFV A2T. These results are in accordance with previous reports suggesting that the A2T plays a role in the positioning of the prothrombin activation sites towards the catalytic triad of FXa[26,33,42]. In sharp contrast to the human system, we observed that the ptFV A2T facilitates prothrombin conversion in the absence of a lipid membrane layer. These findings suggest that the FV A2T plays an important role in the interaction with FXa and prothrombin at physiological phosphatidylserine concentrations (<5%) or in conditions with limiting FXa/membranes[43,44].

Exchange of the A2T resulted in a unique gain-of-function in human FVa by enabling hFVa-ptA2T to bypass the need for membrane binding. Using peptide inhibition studies we identified a potential role for the N-terminal region of the ptFV A2T by facilitating prothrombin activation when anionic membranes are not available. Interestingly, the lipid-independent activity of hFVa-ptA2T was only observed when the cofactor activity was assayed using the protease ptFXa, indicating that the venom-derived FXa comprises an essential element that contributes to the formation of a prothrombinase-like complex in the absence of membranes. Supporting our peptide-based approach, the X-ray structure of Pseutarin C revealed that the N-terminal part of the acidic ptFVa A2T interacts with ptFXa via the highly basic heparin binding site[16], providing evidence that this ptFXa region comprises an essential element that allows for the

formation of a high affinity ptFVa/ptFXa complex in solution. However, global structural comparison of the Pseutarin C structure with the human ternary model did not reveal major conformational alterations in the FXa A2T binding site that could readily explain the different effects between ptFXa and hFXa[16,28] **(Figure S7)**. Future studies focusing on *in silico* analysis of the molecular interactions may provide enhanced insight. In an attempt to identify the responsible structural element, we examined a potential role for the extended 99-loop of ptFXa by experimental assessment of several previously reported FXa variants[17]. However, these variants were unable to support thrombin generation in the absence of anionic membranes (data not shown), excluding a role for this insertion. An alternative explanation might be a structural modification in the Gla domain, which could allosterically influence the conformation of FVa binding sites[42].

Previous work suggests that the increased FVa/FXa affinity upon binding to negatively charged membranes is the result of conformational constraints that increase the chance of productive interactions[41]. Moreover, interaction with anionic membranes was speculated to induce structural rearrangements in the lipid-binding C domains of FVa, resulting in allosteric changes within the FXa binding regions of the A2 domain[42,45]. The latter is supported by two C2 domain crystal structures revealing an 'open' and 'closed' conformation of the phospholipid protruding spikes[46]. In contrast, our data suggest that such structural rearrangements are not essential for prothrombinase assembly since the human variant hFVa-ptA2T was able to engage ptFXa with high affinity in the absence of membranes. Although it is possible that ptFVa or hFVa-ptA2T binding to ptFXa mimics the conformational changes of membrane-bound hFVa, no structural data is available to support this notion.

Our findings further show that introduction of the human A2T in ptFVa results in a reduced cofactor activity upon APC-mediated proteolysis, demonstrating that the ptFV A2T significantly contributes to its functional APC-resistance. Interestingly, substitution of the human Arg679 APC cleavage site in ptFVa-hA2T, thereby rendering it resistant to APC proteolysis, partly rescued the loss of cofactor activity. Considering that the A2T is a long and highly flexible region, it is unlikely that proteolysis at Arg679 destabilizes any region outside of the A2T itself. As such, these results might indicate that the C-terminal part of the ptFV A2T plays a substantial role in the APC-resistance. Based on the available data we hypothesize that the ptFV A2T allows the formation of productive interactions with ptFXa and/or prothrombin. However, these interactions only become functionally relevant in unfavorable conditions, with the cofactor being proteolyzed or in the absence of membranes. This is supported by our observation that the loss of cofactor activity upon APC-mediated proteolysis was not a consequence of A2 domain dissociation. Moreover, no difference in APC inactivation was observed for ptFVa-hA2T

and a variant in which the human APC cleavage region Arg306 was introduced and the disulfide bond connecting the ptFV A2-A3 domains eliminated (ptFVa-hA2T-h306-SS). Collectively, this indicates that ptFVa comprises mechanisms to support ptFXa affinity that are distinct from the essential requirements of mammalian FVa inactivation.

We previously demonstrated that ptFV comprises a rigid A2 domain loop that forms stable interactions with the A1 domain following APC-mediated proteolysis[21]. These interactions might be responsible for preventing A2 domain dissociation and could explain the residual and stable cofactor activity (~15%) of ptFVa-hA2T and ptFVa-hA2T-h306-SS following cleavage by APC. In similar fashion, we recently observed that proteolysis by plasmin significantly reduced the cofactor activity of ptFVa to a residual ~20% cofactor activity[21]. Taken together, our body of work indicates that the ptFV A2T plays an elementary role in the functional resistance to APC, whereas the residual cofactor activity of APC-proteolyzed ptFVa-hA2T or plasmin-proteolyzed ptFVa is a result of the regions that stabilize A2 domain binding.

Translation of the procoagulant enhancements of ptFV to hFV might provide unique opportunities for the generation of novel procoagulant and more stable FV products as potential therapeutic agents for bleeding disorders. Previous reports have demonstrated the efficacy of engineered FVa variants with improved stability in bleeding disorders such as hemophilia[47-50]. Furthermore, the peptide-mediated inhibition of the ptFVa/ptFXa complex suggests that targeting the A2T could be a viable strategy to generate the first specific antidote for envenomation by brown snakes and likely other Elapids[51]. The uncontrolled activation and consumption of the coagulation system that hallmarks VICC[8] follows from the procoagulant action of the FV(a)- and FX(a)-like proteins in brown snake and other snake venoms. A strategy that specifically aims to inhibit these procoagulant effects could therefore significantly improve the efficacy of antidote therapy.

In conclusion, we have identified a unique structural element responsible for the remarkable procoagulant enhancements that have transformed ptFV into a potent hemostatic toxin. Furthermore, by creating a human chimeric variant comprising the ptFV A2T, we have for the first time generated a human FVa molecule that has circumvented the need for membrane binding, one of the hallmarks of coagulation. As such, the ptFV A2T represents the exceptional modifications that are generated by evolutionary pressure to provide selective advantage.

Acknowledgements

This work was financially supported by the Bayer Hemophilia Awards Program (Special Project Award) and Landsteiner Foundation for Blood Transfusion (LSBR, grant. no. 1451). The funding agencies had no role in the preparation, review, or approval of the manuscript.

Figures

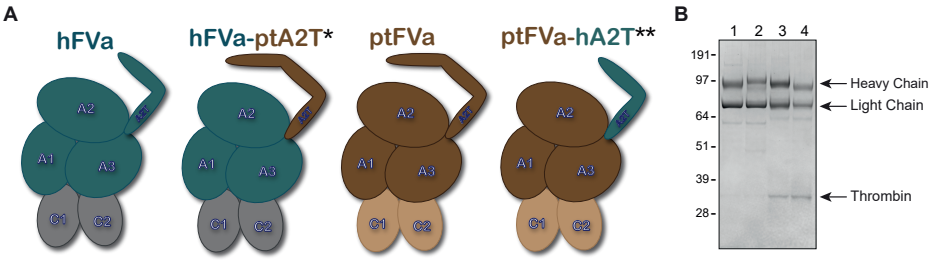

Figure 1. Generation of chimeric FVa variants. (A) Schematic representation of human FVa (hFVa, blue) and venom-derived *P. textilis* FVa (ptFVa, brown). The A2 domain C-terminus (A2T) was swapped between hFV and ptFV, generating hFVa-ptA2T and ptFVa-hA2T. * The human FV A2T region Glu662-Arg709 was replaced for the corresponding ptFV A2T region Gly663-Arg742 since exchange of the complete A2T resulted in a dysfunctional hFV protein due to disruption of the highly conserved C575-C656 disulfide bond. In addition, a hFVa-ptA2T variant in which the complete A2T was exchanged and C656 was reintroduced was generated (hFVa-ptA2T-Y656C). ** ptFVa-hA2T comprises the complete human A2T. Additional Arg680Gln substitution generated ptFVa-hA2T-R679Q. The specific A2T sequences of the FV variants are displayed in **Fig. S1B**. **(B)** SDS-PAGE analysis of purified thrombin-activated FVa variants (2 µg per lane) under reducing conditions and visualized by staining with Coomassie Brilliant Blue R-250. Lane 1, hFVa; lane 2, hFVa-ptA2T; lane 3, ptFVa; lane 4, ptFVa-hA2T. The apparent molecular weights of the standards are indicated on the left. Relevant FVa fragments are indicated on the right.

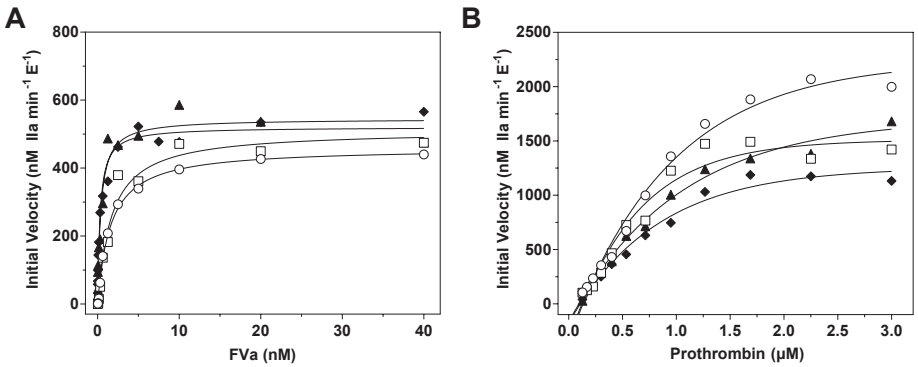

Figure 2. Steady-state kinetics for prothrombinase assembly and prothrombin conversion. **(A)** Reaction mixtures containing 1.4 μM prothrombin, 50 μM PCPS, 10 μM DAPA, and increasing concentrations (0-40 nM) of FVa variant were incubated for 5 min at 25°C. The reaction was initiated with 0.4 nM hFXa (for hFVa and hFVa-ptA2T) or 0.2 nM ptFXa (for ptFVa and ptFVa-hA2T), and thrombin formation was monitored during 3 min as described under "Materials and Methods". **(B)** Reaction mixtures containing 0-3 μM prothrombin, 50 μM PCPS, 10 μM DAPA, and 20 nM FVa variant were incubated for 5 min at 25°C. The reaction was initiated with 0.1 nM hFXa (for hFVa and hFVa-ptA2T) or ptFXa (for ptFVa and ptFVa-hA2T), and thrombin formation was monitored during 3 min as described under "Materials and Methods". The FVa variants are hFVa (open circles), hFVa-ptA2T (open squares), ptFVa (closed diamonds), or ptFVa-hA2T (closed triangles). Kinetic parameters of prothrombin conversion were determined by fitting the data to a Michaelis-Menten function by non-linear regression (Table 1). The data are representative of two to three independent experiments.

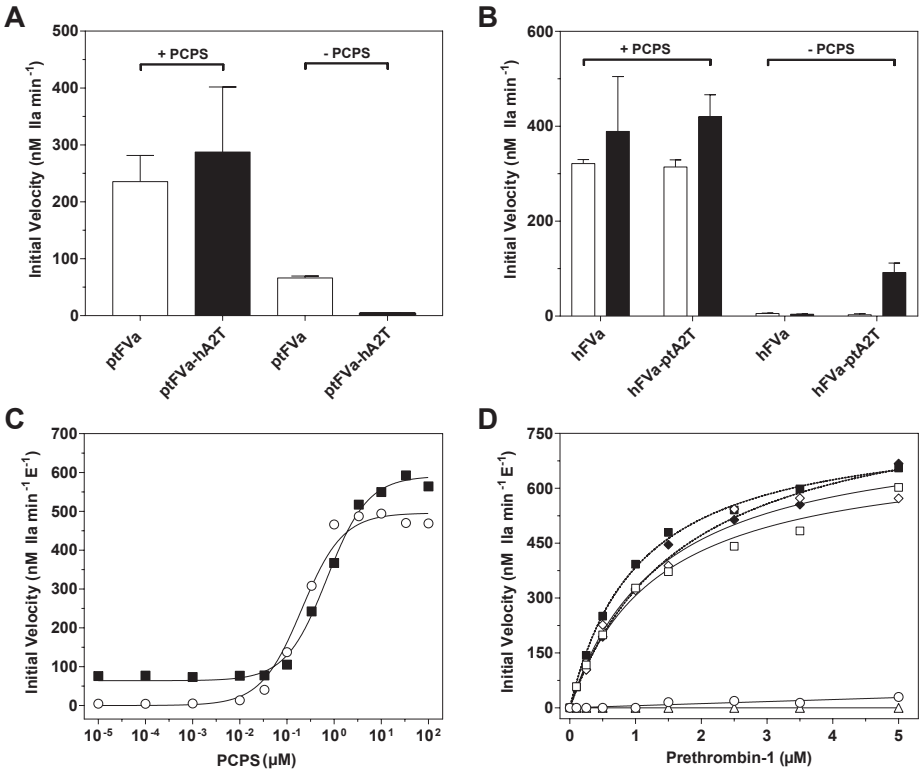

Figure 3. The *P. textilis* factor V A2 domain C-terminus confers lipid-independent prothrombin activation. **(A-B)** Reaction mixtures containing 1.4 μM prothrombin, 10 μM DAPA, and **(A)** 1 nM ptFVa or ptFVa-hA2T, or **(B)** 1 nM hFVa or hFVa-ptA2T were incubated for 5 min at 25°C in the presence or absence of 50 μM PCPS, as indicated. The reaction was initiated with **(A)** 10 nM ptFXa, or **(B)** by 10 nM hFXa (white bars) or ptFXa (black bars) and thrombin generation was monitored during 1.5-5 min as described under "Materials and Methods". **(C)** Initial velocity of thrombin generation determined in reaction mixtures containing 1.4 μM prothrombin, 10 μM DAPA, 1 nM hFVa (open circles) or hFVa-ptA2T (closed squares), 10 nM ptFXa and increasing concentrations of PCPS (0.00001-100 μM). **(D)** Initial velocity of thrombin generation determined in reaction mixtures containing 10 μM DAPA, 1 nM hFVa (circles), hFVa-ptA2T (squares), ptFVa (diamonds), or ptFVa-hA2T (triangles), 10 nM ptFXa, and increasing concentrations of prethrombin-1 in the presence (open symbols) or absence of PCPS (closed symbols; dotted lines). Bars depict mean ± 1 standard deviation. The lines were drawn following nonlinear regression analysis. The data are representative of two to three independent experiments.

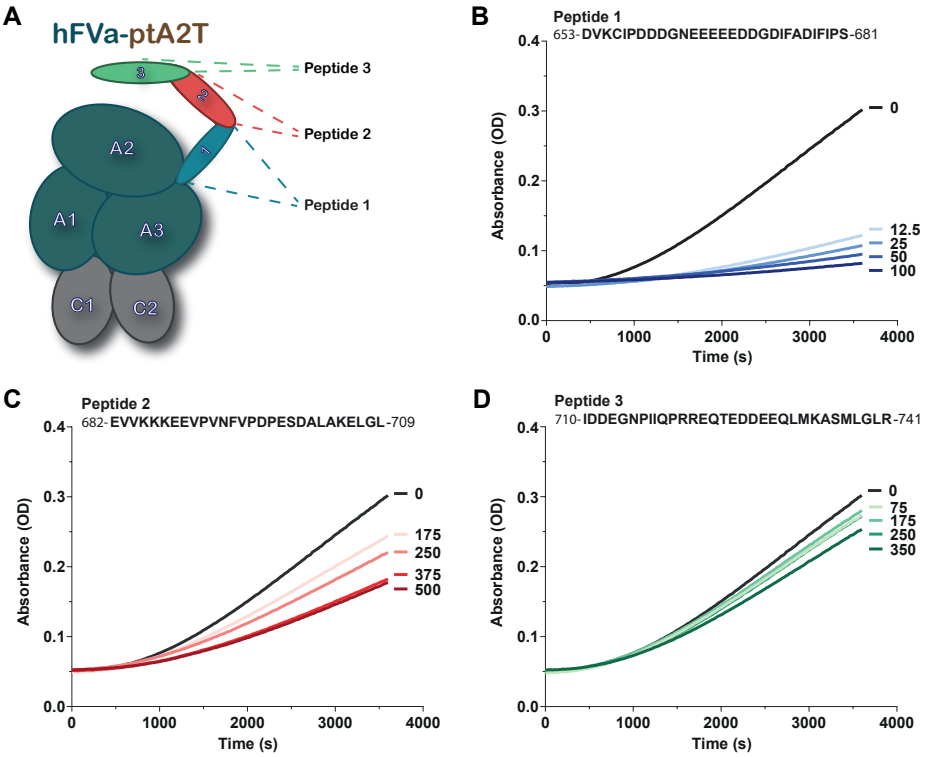

Figure 4. Peptide-mediated inhibition of the lipid-independent prothrombin conversion by the hFVa-ptA2T/ptFXa complex. (A) Schematic representation of ptFVa and the three peptides that represent a specific region of the ptFV A2T. The three A2T regions were selected based on their assumed interactions in the FVa-FXa-prothrombin complex[16]; specifically: peptide 1 may bind FXa/prothrombin, peptide 2 may interact with prothrombin, and peptide 3 appears as an extended region. **(B-D)** Reaction mixtures comprised 1.4 µM prothrombin, 10 µM DAPA, 100 µM S2238, 5 pM hFVa-ptA2T, and indicated concentrations (µM) of either peptide 1 **(E)**, peptide 2 **(F)**, or peptide 3 **(G)**, and prothrombin conversion was initiated by the addition of 10 nM ptFXa. Thrombin formation was continuously monitored during 60 min at 25°C as described under "Materials and Methods", and the absorbance (optical density, OD) at 405 nm representing S2238 hydrolysis was plotted over time. The data are representative of three independent experiments.

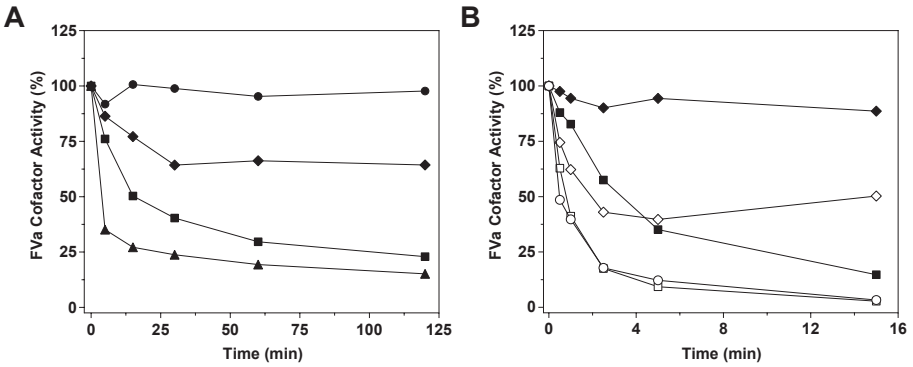

Figure 5. Functional resistance to activated protein C in factor Va variants comprising the *P. textilis* factor V A2 domain C-terminus. (A) Reaction mixtures containing 50 μM PCPS and 500 nM ptFVa (circles), ptFVa-hA2T (squares) ptFVa-hA2T-R679Q (diamonds) or ptFVa-hA2T-h306-SS (triangles) were incubated with 750 nM APC and **(B)** similar mixtures containing hFVa (circles), hFVa-ptA2T (squares) or hFVa-ptA2T-pt306 (diamonds) were incubated with 10 nM APC at 37°C. At selected time intervals, samples were removed for cofactor activity by determination of the initial velocity of prothrombin conversion, initiated by either hFXa (open symbols) or ptFXa (closed symbols). The data are representative of two to three independent experiments.

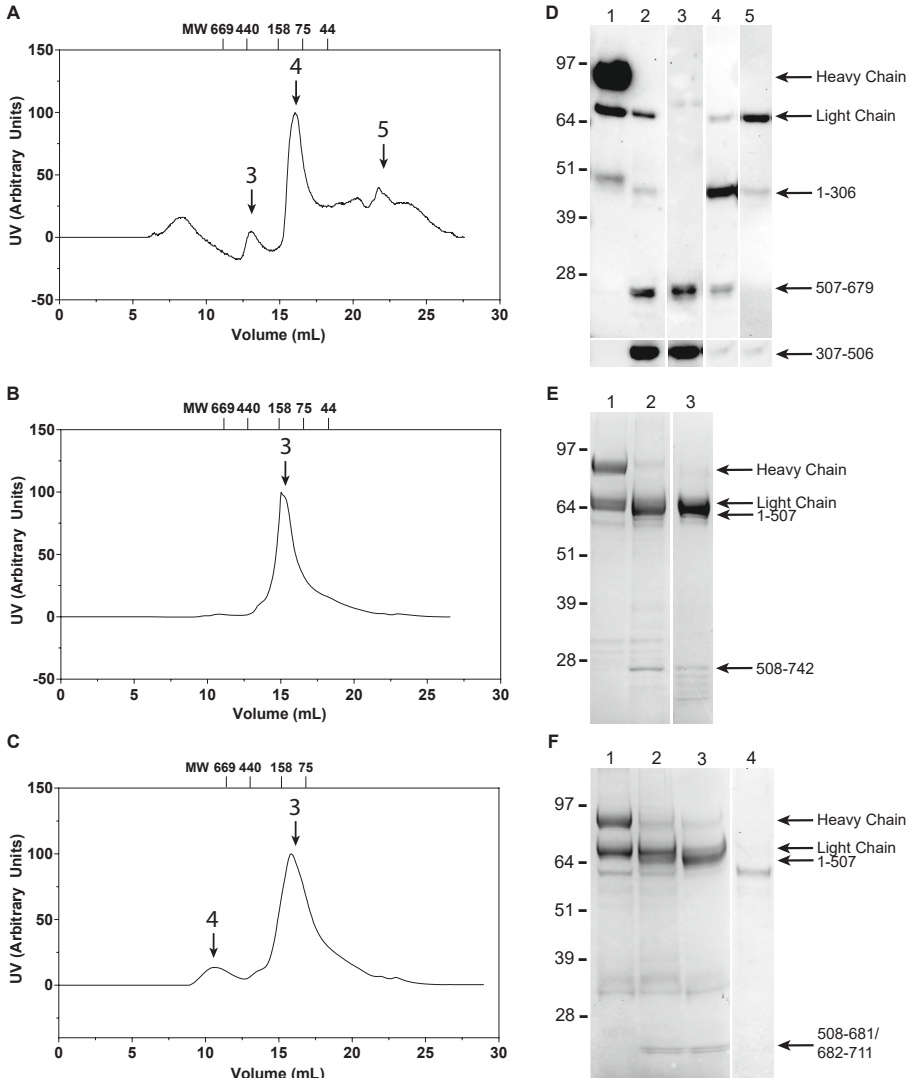

Figure 6. Structural integrity of activated protein C-treated FVa following exchange of the A2T. (A-C) Size-exclusion elution profile of APC-treated hFVa **(A)**, ptFVa **(B)**, or ptFVa-hA2T **(C)** performed as detailed in 'Materials and Methods'. Arrows and numbers indicate the respective fractions shown in **D-F** (**A-B**, data from reference[21]). **(D)** Western blot analysis of hFVa under reducing conditions following proteolysis by APC and size-exclusion chromatography elution. Lane 1, thrombin-activated hFVa; lane 2, APC-treated hFVa; lane 3, A2 domain fraction; lane 4, A1-A3-C1-C2 and A2 domain fraction; lane 5, A1-A3-C1-C2 domains fraction. **(E-F)** SDS-PAGE of APC-treated ptFVa **(E)** or ptFVa-hA2T **(F)** following size-exclusion chromatography under reducing conditions and visualized by staining with Coomassie Brilliant Blue R-250 (**E-F**, data from reference[21]). Lanes 1, thrombin-activated ptFVa variant; lanes 2, APC-treated ptFVa variant; lanes 3 and 4, elution fractions indicated by the black arrows and numbers in **B-C**. The apparent molecular weights of the standards are indicated on the left. Relevant FVa fragments are indicated on the right. Panel **D** and **F** are composed of two Western Blots or SDS-PAGE gels, respectively.

	FXa*	Prothrombinase* - prothrombin		Prothrombinase* – prethrombin-1		FVa/FXa* – prethrombin-1	
	$K_{d,\,app}$ (nM)	K_m (μM)	k_{cat} (min^{-1})	K_m (μM)	k_{cat} (min^{-1})	K_m (μM)	k_{cat} (min^{-1})
hFVa	1.58 ± 0.28[a]	0.47 ± 0.32	2385 ± 541	N.A.	N.A.	N.D.	N.D.
hFVa-ptA2T	1.69 ± 0.69[a]	0.48 ± 0.21	1406 ± 229	1.03 ± 0.53	591 ± 102	1.18 ± 0.17	829 ± 43
ptFVa	0.27 ± 0.08[b]	0.68 ± 0.15	1325 ± 112	1.46 ± 0.76	796 ± 153	1.68 ± 0.66	818 ± 131
ptFVa-hA2T	0.46 ± 0.17[b]	0.71 ± 0.22	1947 ± 426	N.A.	N.A.	N.D.	N.D.

Table 1. Kinetic constants for macromolecular substrate cleavage. The kinetic constants were obtained as described in 'Materials and Methods' in the presence (prothrombinase) or absence (FVa/FXa) of PCPS. Fitted values ± 1 standard deviation of the induced fit are representative of two to three independent experiments. N.D., not determined. N.A., for this experiment, rates were too low to accurately assess kinetic parameters. * The kinetic parameters for hFVa or hFVa-ptA2T were determined using hFXa and for ptFVa or ptFVa-hA2T using ptFXa, respectively.

Supplemental Methods

Materials and Reagents: The inhibitor dansylarginine-N-(3-ethyl-1,5-pentanediyl)amide (DAPA) was from Haematologic Technologies (Essex Junction, VT). The peptidyl substrate H-D-Phe-Pip-Arg-pNA (S2238) was obtained from Instrumentation Laboratories (Bedford, MA, USA). All tissue culture reagents were from Life Technologies (Carlsbad, CA, USA). Small unilamellar phospholipid vesicles (PCPS) composed of 75% (wt/wt) hen egg L-phosphatidylcholine (PC) and 25% (wt/wt) porcine brain L-phosphatidylserine (PS) (Avanti Polar Lipids, Alabaster, AL, USA) were prepared and characterized as described previously[52]. All functional assays were performed in HEPES-buffered saline (HBS: 20 mM HEPES, 0.15 M NaCl, pH 7.5) supplemented with 5 mM $CaCl_2$, 0.1% PEG8000 and filtered over a 0.2 µm filter (assay buffer).

Proteins: The human plasma-derived coagulation factors, prothrombin, α-thrombin, and activated protein C were from Haematologic Technologies (Essex Junction, VT). Restriction endonucleases BbvCI and Bsu36I were obtained from New England Biolabs (Ipswich, MA, USA), while AbsI was purchased from SibEnzyme (Novosibirsk, Russia). Hirudin and phospholipase C were from Sigma-Aldrich (St Louis, MO, USA). Recombinant human (hFXa) and venom-derived *Pseudonaja textilis* FXa (ptFXa) were prepared, purified, and characterized as described[17,53]. Recombinant constitutively active B-domainless human factor V (FV-810; hFV) and venom-derived *P. texilis* FV (ptFV), were prepared, purified, and characterized as described previously[14,34]. The peptides DVKCIPDDDGNEEEEEDDGDIFADIFIPS (designated peptide 1), EVVKKKEEVPVNFVPDPESDALAKELGL (designated peptide 2) and IDDEGNPIIQPRREQTEDDEEQLMKASMLGLR (designated peptide 3) were generated and purchased from Genscript (Piscataway, NJ, USA) and dissolved in ultrapure water or Dulbecco's Phosphate Buffered Saline (Life Technologies, Carlsbad, CA, USA) at 5-10 mg mL^{-1}.

Construction of FV Variants: Initially, we generated constructs encoding for hFV (pED-hFV-810) comprising the venom-derived *P. textilis* A2T, designated pED-hFV-ptA2T$^{(1)}$ (ptFV sequence Gly693-Arg772; Uniprot: Q7SZN0 replacing hFV sequence Glu690-Arg737; Uniprot: P12259), and pED-hFV-ptA2T$^{(2)}$ (ptFV sequence Asp684-Arg772; Uniprot: Q7SZN0 replacing hFV sequence Asp681-Arg737; Uniprot: P12259). Furthermore, we generated ptFV constructs (pED-ptFV) comprising the human A2T sequence named pED-ptFV-hA2T$^{(1)}$ (hFV sequence Ser692-Arg737; Uniprot: P12259, replacing Gly693-Arg772; Uniprot: Q7SZN0) and pED-ptFV-hA2T$^{(2)}$ (hFV sequence Asp681-Arg737; Uniprot: P12259, replacing Asp684-Arg772; Uniprot: Q7SZN0). The constructs were generated by restriction enzyme digestion (hFV-ptA2T, BbvCI and AbsI;

ptFV-hA2T, BbvCI and Bsu36I) of pUC57 plasmids encoding the specifically designed FV A2T region flanked by pED-hFV-810 or pED-ptFV nucleotides, which were generated and purchased from Genscript (Piscataway, NJ, USA). The digested product was gel-purified and subcloned in pED vectors using identical restriction enzymes. Upon transfection, the variants hFV-ptA2T$^{(2)}$ and ptFV-hA2T$^{(1)}$ were not secreted or did not display FV activity. We were able to rescue expression of hFV-ptA2T$^{(2)}$ by Tyr656Cys (Tyr707; Uniprot: Q7SZN0) substitution, designated as pED-hFV-ptA2T-Y656C, since in hFV this cysteine forms a highly conserved disulfide bond with Cys575 (Cys603; Uniprot: P12259). pED-hFV-ptA2T-Y656C was generated from pED-ptFV-hA2T$^{(2)}$ by employing mutagenic complementary oligonucleotides (primers, tgatgatgaagatgagggaaatg and caattggcatccctgaatttcag) using the Q5® Site-Directed Mutagenesis Kit (New England Biolabs, Ipswich, MA, USA) according to manufacturer's protocol. The constructs pED-hFV-ptA2T$^{(1)}$ and pED-ptFV-hA2T$^{(2)}$ were subsequently used for the generation of pED-hFV-ptA2T-pt306 and pED-ptFV-hA2T-h306-SS by substitution of the Arg306 region (human full-length FV sequence Pro302-Leu308; Uniprot: P12259. ptFV sequence Gly303-Thr309; Uniprot: Q7SZN0) and deletion of ptFV's unique disulfide bond (ptFV residues Cys642 and Cys1002[16]; Uniprot: Q7SZN0). The variant pED-hFV-ptA2T-pt306 was generated using a pUC57 plasmid encoding pED-ptFV nucleotides 2124-2144, flanked by pED-hFV nucleotides, which was generated and purchased from Genscript (Piscataway, NJ, USA). The resulting pUC57 plasmid was digested with XcmI and Bsu36I, gel-purified, and subcloned into pED-hFV-ptA2T via digestion with the same enzymes. For pED-ptFV-hA2T-h306-SS, first pED-ptFV-hA2T-h306 was generated by employing mutagenic complementary oligonucleotides (primers, caggaatcttagaaagttatcctttagagaac and gttttctttggacagtctttgatatttagataacc) as described[21]. Subsequently, the residues encoding ptFV's unique disulfide bond were substituted (primers Cys642Ser, tgagatgagcaatggcatgagattg and gaggagccccatgatgacagaag; primers Cys1002Ser, gaagagaaacttataggagtccaatc and agaagtgcttttgtcagattttgg) to generate pED-ptFV-hA2T-h306-SS using the Q5® Site-Directed Mutagenesis Kit (New England Biolabs, Ipswich, MA, USA) according to manufacturer's protocol. Additionally, we used pED-ptFV-hA2T$^{(2)}$ to generate the construct pED-ptFV-hA2T-R679Q comprising a Arg679Gln substitution (Arg707; Uniprot: P12259). (primers, caggaatcttagaaagttatcctttagagaac and gttttctttggacagtctttgatatttagataacc) employing the Q5® Site-Directed Mutagenesis Kit.

Expression and purification of FV variants: Transfection of the plasmids encoding FV constructs into baby hamster kidney cells, the selection of stable clones, and the expression and purification of hFV and ptFV were performed as described previously[14,34]. Briefly, FV proteins were purified employing ion-exchange chromatography on a Q-Sepharose FF column (GE Healthcare) using a NaCl elution gradient in HBS supplemented with 5 mM $CaCl_2$ and 1 mM BZA, pH 7.4. Fractions containing FV activity

were pooled and dialyzed versus 20 mM HEPES, 5mM $CaCl_2$, pH 7.4 for human FV variants and 20 mM MES, 5 mM $CaCl_2$, pH 6.0 for ptFV variants, loaded on a POROS HQ/20 (hFV) or HS/20 column (ptFV) (Applied Biosystems) and eluted using a NaCl gradient. Protein purity was assessed by SDS-PAGE using pre-cast 4%–12% gradient gels under nonreducing and reducing conditions (50mM DTT) using the MOPS buffer system (Life technologies; Carlsbad, CA, USA) followed by staining with Coomassie Brilliant Blue R-250. For pretreatment with thrombin, FV variants were incubated for 15 minutes with α-thrombin (molar ratio 15:1 for hFV or 3.75:1 for ptFV) in assay buffer at 37°C, followed by the addition of a 10-fold molar excess of hirudin. Following transfection and purification, the protein variants generated by pED-hFV-ptA2T[(1)] and pED-ptFV-hA2T[(2)] were designated as hFV-ptA2T and ptFV-hA2T, respectively. The molecular weight of the newly generated variants was assumed as follows, hFV-ptA2T, hFV-ptA2T-Y656C, and hFV-ptA2T-pt306: 220,000 kDa; ptFV-hA2T, ptFV-hA2T-R679Q, and ptFV-hA2T-h306-SS: 159,000 kDa[14,34]. The extinction coefficients (E0.1%, 280 nm) of the FV variants were assumed to be equal to hFV (1.54) and ptFV (1.25), respectively[14,34].

Supplemental Figures

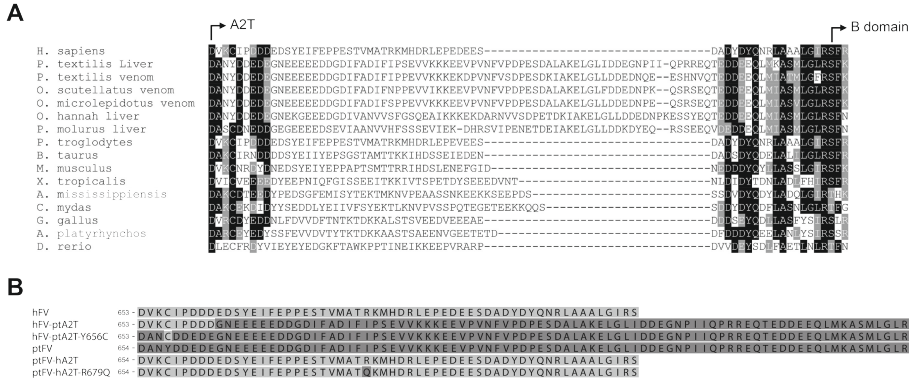

Supplementary figure 1. (A) Alignment of the amino acid sequences comprising the FV A2 domain C-terminus (A2T) (Clustal Omega Module; EMBL-EBI, UK). Residues identical to the column consensus are shown in black; residues similar to the column consensus are shown in grey. The start of A2T and the B domain are indicated. **(B)** Sequence alignment defining the A2T of the generated recombinant FV variants. Human A2T residues are shown in blue, ptFV A2T residues are shown in brown.

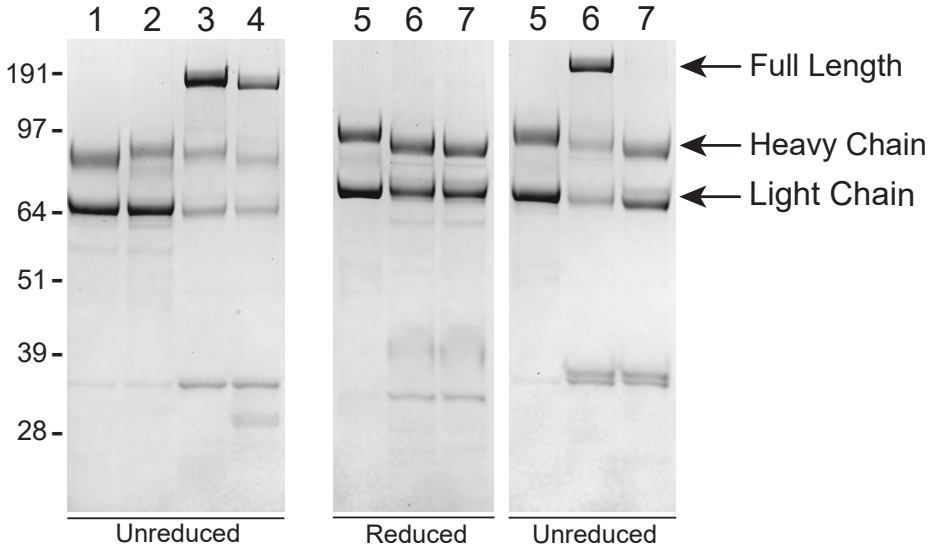

Supplementary figure 2. SDS-PAGE of FVa variants. SDS-PAGE analysis of purified thrombin-activated FVa variants (2 µg per lane) under reducing and non-reducing conditions, visualized by staining with Coomassie Brilliant Blue R-250. Lane 1, hFVa; lane 2, hFVa-ptA2T; lane 3, ptFVa; lane 4, ptFVa-hA2T; lanes 5, hFVa-ptA2T-pt306; lanes 6, ptFVa-hA2T-h306; lanes 7, ptFVa-hA2T-h306-SS. The apparent molecular weights of the standards are indicated on the left. Relevant FVa fragments are indicated on the right.

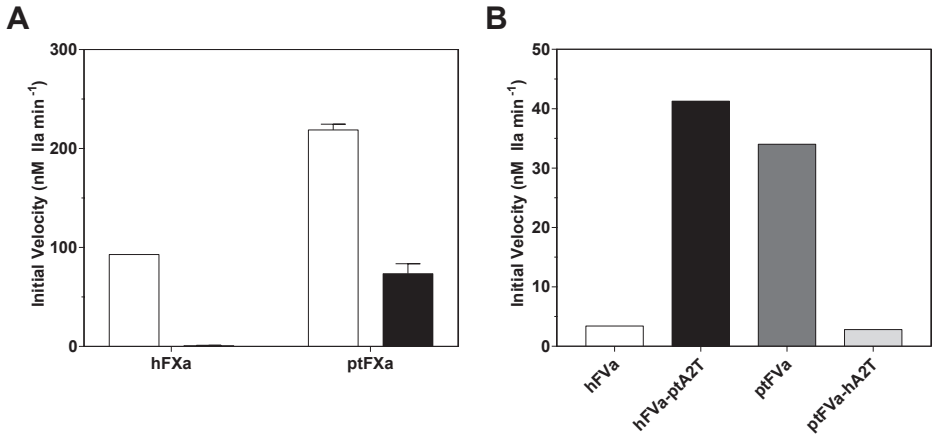

Supplementary Figure 3. Lipid-independent prothrombin conversion. (A) The initial velocity of thrombin generation was determined in the presence of 1.4 μM prothrombin, 10 μM DAPA, 1 nM hFVa-ptA2T-Y656C and 10 nM hFXa or ptFXa in the presence (open bars) or absence (closed bars) of PCPS (50 μM). **(B)** Mixtures containing 12.5 nM FVa variant and 125 μM PCPS were incubated with phospholipase C (25 U/mL) for 10 min at 37°C. Samples were removed for cofactor activity by determination of the initial velocity of thrombin generation in reaction mixtures containing 1.4 μM prothrombin, 10 μM DAPA, 10 nM ptFXa, 1 nM phospholipase C-treated hFVa, hFVa-ptA2T, ptFVa or ptFVa-hA2T. Bars depict mean ± 1 standard deviation for one to three independent experiments.

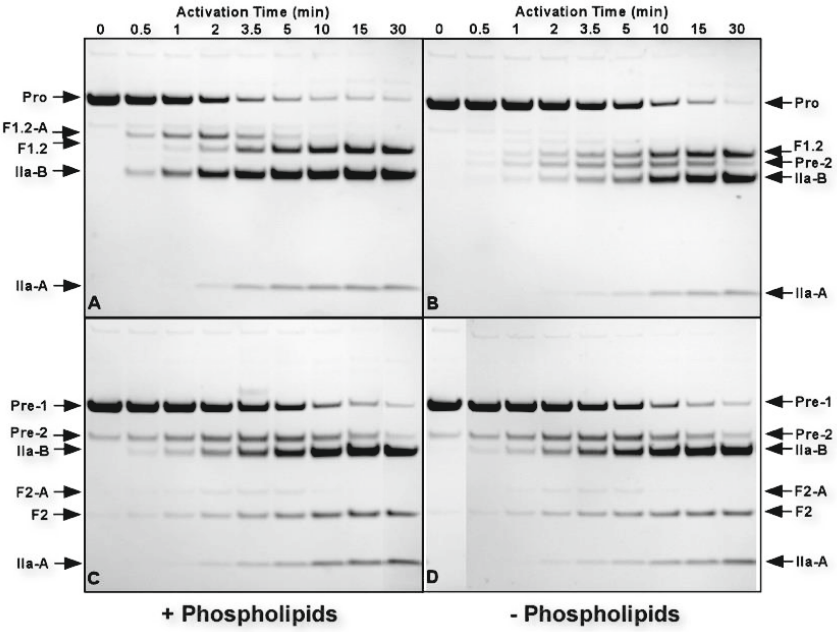

Supplementary Figure 4. Macromolecular substrate cleavage by ptFV-ptFXa. At the indicated time points samples were taken from reaction mixtures containing 5.4 mM prothrombin (panels A,B) or prethrombin-1 (panels C,D), 1 nM ptFXa, and 30 nM ptFV with (panels A,C) or without (panels B,D) 30 mM PCPS present. Samples were quenched, subjected to SDS-PAGE under reducing conditions, and visualized by staining with Coomassie Brilliant Blue R-250. Identities of the relevant species are indicated next to the gels, and time point 0 in panel D is taken from panel C. The proteins used in this assay were gifted by Dr. Camire (Children's Hospital of Philadelphia, Philadelphia, United States).

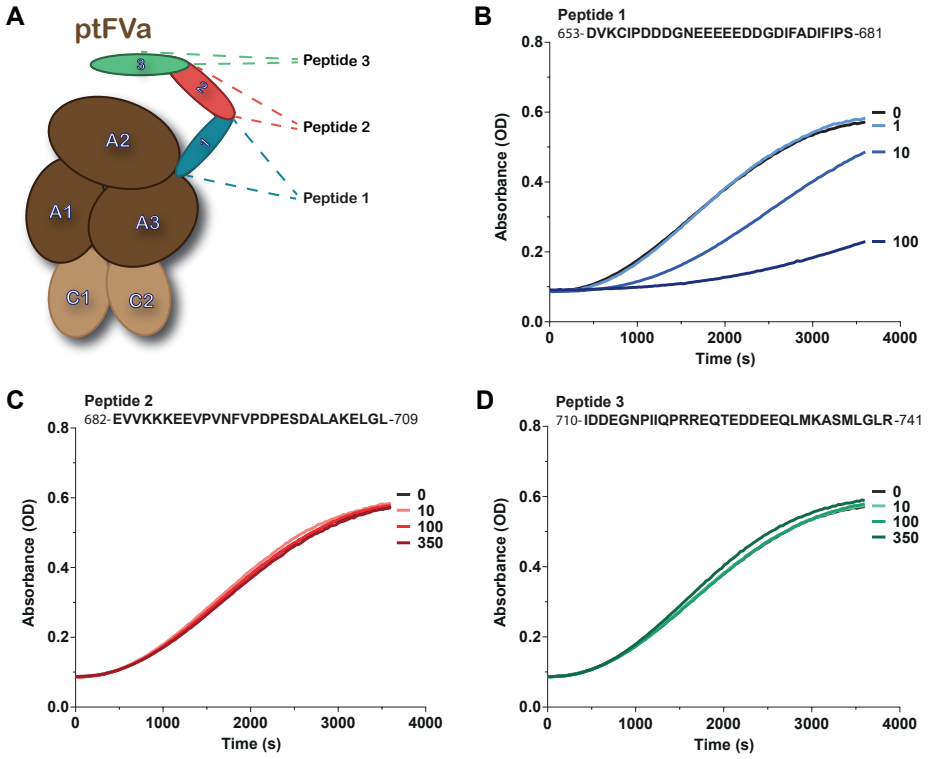

Supplementary figure 5. Peptide-mediated inhibition of the lipid-independent prothrombin conversion by the ptFVa/ptFXa complex. (A) Schematic representation of ptFVa and the three peptides that represent a specific region of the ptFV A2T. The three A2T regions were selected based on their hypothesized interaction in the FVa-FXa-prothrombin complex. **(B-D)** Inhibition of ptFVa/ptFXa activity using peptides comprising parts of the ptFV A2T in a continuous assay. Reaction mixtures containing 1.4 μM prothrombin, 10 μM DAPA, 100 μM S2238, 5 pM ptFVa and indicated concentrations of either peptide 1 **(B)**, peptide 2 **(C)**, or peptide 3 **(D)** were initiated by 10 nM ptFXa. Thrombin formation was continuously monitored during 1.5-5 min as described under "Materials and Methods". The data are representative of two independent experiments.

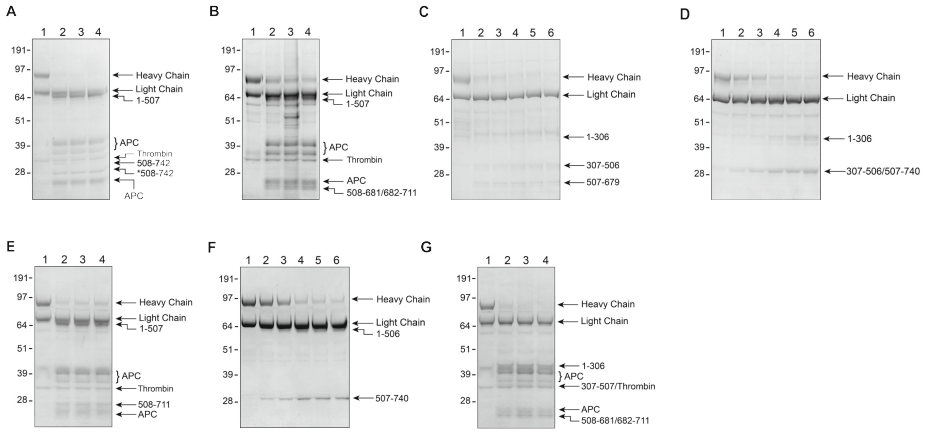

Supplementary figure 6. Activated protein C treatment of human and *P. textilis* factor Va variants. SDS-PAGE of APC-treated **(A)** ptFVa, **(B)** ptFVa-hA2T, **(C)** hFVa, **(D)** hFVa-ptA2T, **(E)** ptFVa-hA2T-R679Q, **(F)** hFVa-ptA2T-pt306, and **(G)** ptFVa-hA2T-h306-SS (3 µg per lane) under reducing conditions and visualized by staining with Coomassie Brilliant Blue R-250. **(A, B, E, G)** Lanes 1-4 represent time samples quenched at 0, 30, 60, and 120 min. **(C, D, F)** Lanes 1-6 represent time samples quenched at 0, 0.5, 1, 2.5, 5, and 15 min. The apparent molecular weights of the standards are indicated on the left. Relevant FVa fragments are indicated on the right. We hypothesize that *508-742 is cleaved at a C-terminal position because its N-terminal sequence was determined to be the same as 508-742[21].

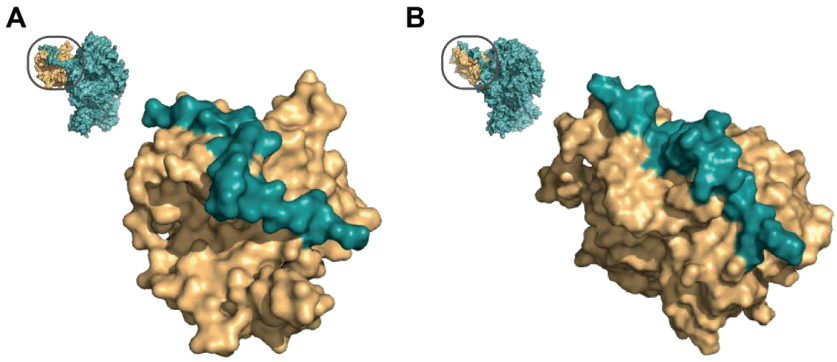

Supplementary figure 7. Interface between the factor Va A2 domain C-terminus and factor Xa. (A) A zoomed-in region of the Pseutarin C crystal structure[16] or **(B)** the human ternary model by Shim *et al.* is shown[28]; the insert outlines the specific region depicted. The FVa A2T is shown in teal, the serine protease domain of FXa is depicted in yellow. The additional FVa regions, the FXa light chain, and prothrombin have been removed for clarity.

	K_m μM	K_{cat} min^{-1}
+ PCPS	1.1 ± 0.1	1610 ± 28
- PCPS	1.1 ± 0.1	1570 ± 38
- $CaCl_2$	1.9 ± 0.2	530 ± 12
+ EDTA	2.6 ± 0.5	350 ± 21

Supplementary Table 1. Kinetic constants for prethrombin-1 cleavage. The initial velocity of thrombin generation was determined at increasing concentrations of prethrombin-1 with 0.1 nM ptFXa and 20 nM ptFV. Substrate cleavage was assayed in the presence (+ PCPS) or absence (- PCPS) of 50 μM phospholipid vesicles; under the latter conditions, 5 mM CaCl2 was omitted from the reaction mixture (- CaCl2), or, additionally, 50 mM EDTA (+ EDTA) was added. Data sets were analyzed, and the fitted constants are shown. The data are representative of two similar experiments. The proteins used in this assay were gifted by Dr. Camire (Children's Hospital of Philadelphia, Philadelphia, United States).

References

1 Fry, B. G. Structure-function properties of venom components from Australian elapids. *Toxicon* **37**, 11-32, doi:10.1016/s0041-0101(98)00125-1 (1999).
2 Tans, G. & Rosing, J. Snake venom activators of factor X: an overview. *Haemostasis* **31**, 225-233, doi:10.1159/000048067 (2001).
3 Rao, V. S. & Kini, R. M. Pseutarin C, a prothrombin activator from Pseudonaja textilis venom: its structural and functional similarity to mammalian coagulation factor Xa-Va complex. *Thrombosis and haemostasis* **88**, 611-619 (2002).
4 Kini, R. M. The intriguing world of prothrombin activators from snake venom. *Toxicon* **45**, 1133-1145, doi:10.1016/j.toxicon.2005.02.019 (2005).
5 Berling, I. & Isbister, G. K. Hematologic effects and complications of snake envenoming. *Transfus Med Rev* **29**, 82-89, doi:10.1016/j.tmrv.2014.09.005 (2015).
6 Masci, P. P., Rowe, E. A., Whitaker, A. N. & de Jersey, J. Fibrinolysis as a feature of disseminated intravascular coagulation (DIC) after Pseudonaja textilis textilis envenomation. *Thromb Res* **59**, 859-870, doi:10.1016/0049-3848(90)90399-w (1990).
7 Isbister, G. K. Procoagulant snake toxins: laboratory studies, diagnosis, and understanding snakebite coagulopathy. *Semin Thromb Hemost* **35**, 93-103, doi:10.1055/s-0029-1214152 (2009).
8 Isbister, G. K. *et al.* Factor deficiencies in venom-induced consumption coagulopathy resulting from Australian elapid envenomation: Australian Snakebite Project (ASP-10). *J Thromb Haemost* **8**, 2504-2513, doi:10.1111/j.1538-7836.2010.04050.x (2010).
9 Johnston, C. I. *et al.* The Australian Snakebite Project, 2005-2015 (ASP-20). *Med J Aust* **207**, 119-125, doi:10.5694/mja17.00094 (2017).
10 Rao, V. S., Swarup, S. & Kini, R. M. The nonenzymatic subunit of pseutarin C, a prothrombin activator from eastern brown snake (Pseudonaja textilis) venom, shows structural similarity to mammalian coagulation factor V. *Blood* **102**, 1347-1354, doi:10.1182/blood-2002-12-3839 (2003).
11 Minh Le, T. N., Reza, M. A., Swarup, S. & Kini, R. M. Gene duplication of coagulation factor V and origin of venom prothrombin activator in Pseudonaja textilis snake. *Thrombosis and haemostasis* **93**, 420-429, doi:10.1160/TH04-11-0707 (2005).
12 Rao, V. S., Swarup, S. & Manjunatha Kini, R. The catalytic subunit of pseutarin C, a group C prothrombin activator from the venom of Pseudonaja textilis, is structurally similar to mammalian blood coagulation factor Xa. *Thrombosis and haemostasis* **92**, 509-521, doi:10.1160/TH04-03-0144 (2004).
13 Reza, M. A., Minh Le, T. N., Swarup, S. & Manjunatha Kini, R. Molecular evolution caught in action: gene duplication and evolution of molecular isoforms of prothrombin activators in Pseudonaja textilis (brown snake). *J Thromb Haemost* **4**, 1346-1353, doi:10.1111/j.1538-7836.2006.01969.x (2006).
14 Bos, M. H. *et al.* Venom factor V from the common brown snake escapes hemostatic regulation through procoagulant adaptations. *Blood* **114**, 686-692, doi:10.1182/blood-2009-02-202663 (2009).
15 Bos, M. H. & Camire, R. M. Procoagulant adaptation of a blood coagulation prothrombinase-like enzyme complex in australian elapid venom. *Toxins (Basel)* **2**, 1554-1567, doi:10.3390/toxins2061554 (2010).
16 Lechtenberg, B. C. *et al.* Crystal structure of the prothrombinase complex from the venom of Pseudonaja textilis. *Blood* **122**, 2777-2783, doi:10.1182/blood-2013-06-511733 (2013).
17 Verhoef, D. *et al.* Engineered factor Xa variants retain procoagulant activity independent of direct factor Xa inhibitors. *Nat Commun* **8**, 528, doi:10.1038/s41467-017-00647-9 (2017).

18 Schreuder, M. *et al.* Evolutionary adaptations in Pseudonaja textilis venom factor X induce zymogen activity and resistance to the intrinsic tenase complex. *Accepted in Thrombosis and Haemostasis* (2020).
19 Bos, M. H. & Camire, R. M. A bipartite autoinhibitory region within the B-domain suppresses function in factor V. *J Biol Chem* **287**, 26342-26351, doi:10.1074/jbc.M112.377168 (2012).
20 Bunce, M. W., Bos, M. H., Krishnaswamy, S. & Camire, R. M. Restoring the procofactor state of factor Va-like variants by complementation with B-domain peptides. *J Biol Chem* **288**, 30151-30160, doi:10.1074/jbc.M113.506840 (2013).
21 Schreuder, M., Verhoef, D., Cheung, K. L., Reitsma, P. H. & Bos, M. H. A. *Pseudonaja textilis* Factor Va Retains Structural Integrity and Cofactor Function. *Research and Practice in Thrombosis and Haemostasis* **3**, PB0626 (2019).
22 Bakker, H. M. *et al.* Functional properties of human factor Va lacking the Asp683-Arg709 domain of the heavy chain. *J Biol Chem* **269**, 20662-20667 (1994).
23 Kalafatis, M., Beck, D. O. & Mann, K. G. Structural requirements for expression of factor Va activity. *J Biol Chem* **278**, 33550-33561, doi:10.1074/jbc.M303153200 (2003).
24 Beck, D. O., Bukys, M. A., Singh, L. S., Szabo, K. A. & Kalafatis, M. The contribution of amino acid region ASP695-TYR698 of factor V to procofactor activation and factor Va function. *J Biol Chem* **279**, 3084-3095, doi:10.1074/jbc.M306850200 (2004).
25 Bukys, M. A., Kim, P. Y., Nesheim, M. E. & Kalafatis, M. A control switch for prothrombinase: characterization of a hirudin-like pentapeptide from the COOH terminus of factor Va heavy chain that regulates the rate and pathway for prothrombin activation. *J Biol Chem* **281**, 39194-39204, doi:10.1074/jbc.M604482200 (2006).
26 Hirbawi, J., Bukys, M. A., Barhoover, M. A., Erdogan, E. & Kalafatis, M. Role of the acidic hirudin-like COOH-terminal amino acid region of factor Va heavy chain in the enhanced function of prothrombinase. *Biochemistry* **47**, 7963-7974, doi:10.1021/bi800593k (2008).
27 Schreuder, M., Reitsma, P. H. & Bos, M. H. A. Blood coagulation factor Va's key interactive residues and regions for prothrombinase assembly and prothrombin binding. *J Thromb Haemost* **17**, 1229-1239, doi:10.1111/jth.14487 (2019).
28 Shim, J. Y., Lee, C. J., Wu, S. & Pedersen, L. G. A model for the unique role of factor Va A2 domain extension in the human ternary thrombin-generating complex. *Biophysical chemistry* **199**, 46-50, doi:10.1016/j.bpc.2015.02.003 (2015).
29 Higgins, D. L. & Mann, K. G. The interaction of bovine factor V and factor V-derived peptides with phospholipid vesicles. *J Biol Chem* **258**, 6503-6508 (1983).
30 Camire, R. M. Prothrombinase assembly and S1 site occupation restore the catalytic activity of FXa impaired by mutation at the sodium-binding site. *J Biol Chem* **277**, 37863-37870, doi:10.1074/jbc.M203692200 (2002).
31 Toso, R. & Camire, R. M. Removal of B-domain sequences from factor V rather than specific proteolysis underlies the mechanism by which cofactor function is realized. *J Biol Chem* **279**, 21643-21650, doi:10.1074/jbc.M402107200 (2004).
32 Krishnaswamy, S. & Walker, R. K. Contribution of the prothrombin fragment 2 domain to the function of factor Va in the prothrombinase complex. *Biochemistry* **36**, 3319-3330, doi:10.1021/bi9623993 (1997).
33 Kalafatis, M. & Mann, K. G. The role of the membrane in the inactivation of factor va by plasmin. Amino acid region 307-348 of factor V plays a critical role in factor Va cofactor function. *J Biol Chem* **276**, 18614-18623, doi:10.1074/jbc.M007134200 (2001).
34 Toso, R. & Camire, R. M. Role of Hirudin-like factor Va heavy chain sequences in prothrombinase function. *J Biol Chem* **281**, 8773-8779, doi:10.1074/jbc.M511419200 (2006).
35 Mann, K. G., Nesheim, M. E., Hibbard, L. S. & Tracy, P. B. The role of factor V in the assembly of the prothrombinase complex. *Ann N Y Acad Sci* **370**, 378-388, doi:10.1111/j.1749-6632.1981.tb29750.x (1981).

36 Hirbawi, J., Vaughn, J. L., Bukys, M. A., Vos, H. L. & Kalafatis, M. Contribution of amino acid region 659-663 of Factor Va heavy chain to the activity of factor Xa within prothrombinase. *Biochemistry* **49**, 8520-8534, doi:10.1021/bi101097t (2010).
37 Toso, R., Zhu, H. & Camire, R. M. The conformational switch from the factor X zymogen to protease state mediates exosite expression and prothrombinase assembly. *J Biol Chem* **283**, 18627-18635, doi:10.1074/jbc.M802205200 (2008).
38 Gilbert, G. E., Novakovic, V. A., Kaufman, R. J., Miao, H. & Pipe, S. W. Conservative mutations in the C2 domains of factor VIII and factor V alter phospholipid binding and cofactor activity. *Blood* **120**, 1923-1932, doi:10.1182/blood-2012-01-408245 (2012).
39 Krishnaswamy, S. Exosite-driven substrate specificity and function in coagulation. *J Thromb Haemost* **3**, 54-67, doi:10.1111/j.1538-7836.2004.01021.x (2005).
40 Bradford, H. N., Orcutt, S. J. & Krishnaswamy, S. Membrane binding by prothrombin mediates its constrained presentation to prothrombinase for cleavage. *J Biol Chem* **288**, 27789-27800, doi:10.1074/jbc.M113.502005 (2013).
41 Norstrom, E., Thorelli, E. & Dahlback, B. Functional characterization of recombinant FV Hong Kong and FV Cambridge. *Blood* **100**, 524-530, doi:10.1182/blood-2002-02-0343 (2002).
42 Krishnaswamy, S., Jones, K. C. & Mann, K. G. Prothrombinase complex assembly. Kinetic mechanism of enzyme assembly on phospholipid vesicles. *J Biol Chem* **263**, 3823-3834 (1988).
43 Mann, K. G., Nesheim, M. E., Church, W. R., Haley, P. & Krishnaswamy, S. Surface-dependent reactions of the vitamin K-dependent enzyme complexes. *Blood* **76**, 1-16 (1990).
44 Qureshi, S. H., Yang, L., Manithody, C. & Rezaie, A. R. Membrane-dependent interaction of factor Xa and prothrombin with factor Va in the prothrombinase complex. *Biochemistry* **48**, 5034-5041, doi:10.1021/bi900240g (2009).
45 Bevers, E. M., Comfurius, P. & Zwaal, R. F. Changes in membrane phospholipid distribution during platelet activation. *Biochim Biophys Acta* **736**, 57-66 (1983).
46 Heemskerk, J. W., Bevers, E. M. & Lindhout, T. Platelet activation and blood coagulation. *Thrombosis and haemostasis* **88**, 186-193 (2002).
47 Majumder, R., Quinn-Allen, M. A., Kane, W. H. & Lentz, B. R. A phosphatidylserine binding site in factor Va C1 domain regulates both assembly and activity of the prothrombinase complex. *Blood* **112**, 2795-2802, doi:10.1182/blood-2008-02-138941 (2008).
48 Macedo-Ribeiro, S. *et al.* Crystal structures of the membrane-binding C2 domain of human coagulation factor V. *Nature* **402**, 434-439, doi:10.1038/46594 (1999).
49 Schlachterman, A. *et al.* Factor V Leiden improves in vivo hemostasis in murine hemophilia models. *J Thromb Haemost* **3**, 2730-2737, doi:10.1111/j.1538-7836.2005.01639.x (2005).
50 von Drygalski, A. *et al.* Improved hemostasis in hemophilia mice by means of an engineered factor Va mutant. *J Thromb Haemost* **12**, 363-372, doi:10.1111/jth.12489 (2014).
51 van 't Veer, C. *et al.* An in vitro analysis of the combination of hemophilia A and factor V(LEIDEN). *Blood* **90**, 3067-3072 (1997).
52 Bos, M. H., Meijerman, D. W., van der Zwaan, C. & Mertens, K. Does activated protein C-resistant factor V contribute to thrombin generation in hemophilic plasma? *J Thromb Haemost* **3**, 522-530, doi:10.1111/j.1538-7836.2005.01181.x (2005).
53 Zdenek, C. N. *et al.* Coagulotoxic effects by brown snake (Pseudonaja) and taipan (Oxyuranus) venoms, and the efficacy of a new antivenom. *Toxicol In Vitro* **58**, 97-109, doi:10.1016/j.tiv.2019.03.031 (2019).